



PROJECT ACRONYM
CUPIDO

PROJECT TITLE
Cardio Ultraefficient nanoParticles for Inhalation of Drug prOducts

Deliverable 4.1

Distribution of electromagnetic fields in the target area due to the drug targeting systems

CALL ID	H2020-NMBP-2016-2017		
GA No.	720834		
COORDINATING PERSON	Paolo Ravazzani Email: paolo.ravazzani@ieiit.cnr.it		
NATURE	Report (R)	DISSEMINATION LEVEL	PU
DUE DATE	[31/01/2018]	ACTUAL DELIVERY DATE	[02/02/2018]



AUTHOR(S)

[Serena Fiocchi], [Marta Parazzini], [Paolo Ravazzani]

Table of Revisions

REVISION NO.	DATE	WORK PERFORMED	CONTRIBUTOR(S)
1	[09/01/2018]	Draft document	CNR IEIT
2	[10/01/2018]	Document revision	Kristian Sendstad
3	[11/01/2018]	Document revision	Daniele Catalucci
4	[14/01/2018]	Document revision	CNR IEIT
5	[15/01/2018]	Document revision	Daniele Catalucci
6	[30/01/2018]	Document revision	IPR Team
7	[31/01/2018]	Document revision	CNR IEIT



Table of Contents

1. Executive summary	5
2. Cooperation between participants	6
3. Computational simulations of electromagnetic fields on heart tissues	7
3.1. Introduction	7
3.1.1. Objectives.....	7
3.2. Material and Methods	8
3.2.1. Magnetic targeting system (MTS).....	8
3.2.1.1. Modelling of Magnetic fields and Forces.....	8
3.2.2. Blood Forces	9
3.2.3. Target area definition	9
3.2.1.2. Target area definition in humans	10
3.2.1.3. Target area definition in small animals	11
3.2.4. Magnetic targeting system (MTS) and simulation details	11
3.3. Results.....	11
3.3.1. Magnetic force in mice	11
3.3.2. Magnetic force in humans	12
4. Conclusions	13
5. References	14



Index of Figures and Tables

Figure 1 Coronary blood flow (left) and aorta blood velocity (right) during a cardiac cycle. Redrawn from Hall [2011]	10
Figure 2 Pictorial representation of the Helmholtz+Maxwell coils system	12



1. Executive summary

Scope of the present deliverable was to analyze and compare the feasibility of different magnetic targeting systems (MTS) in generating a magnetic force able to compete with the blood drag force, thus enhancing the absorption of magnetic nanoparticles ($^{Fe}CaPs$) in the heart tissue. This was performed through a computational based approach that includes:

- the target area definition on both a mouse model and nine realistic anatomical human voxel models;
- the resolution of Maxwell's equation to determine the spatial magnetic field distribution at the heart level;
- the calculation of spatial-gradient magnetic fields and magnetic forces in the target area.

The maximum magnetic force that different systems based on either permanent magnets or coils can exert on different ^{Fe}CaP agglomerates were numerically compared to the corresponding maximum and minimum blood drag forces. Based on this analysis, the best technical MTS solution was found and its feasibility was evaluated. Results indicate that:

- for mice, MTS based on small magnets are capable to generate enough force to enhance the absorption of a large fraction of magnetic $^{Fe}CaPs$ through coronary capillaries walls.
- for humans, actual commercially available magnet based systems (with an optimum radius depending of the individual anatomy) represent the best solution in terms of possible depth of targeting, cost, complexity and ease-of-use. They allow attracting and slow $^{Fe}CaPs$ towards anterior and superficial coronary capillaries walls.

Key deliverable achievements:

1. Simulations and comparison of the different magnetic targeting systems that should be able to generate the magnetic force needed to enhance the absorption of magnetic nanoparticles ($^{Fe}CaPs$) in the heart tissues through a computational based approach.
2. Distribution of the magnetic field and the magnetic force due to the different MTS on heart tissues of anatomical human models of different age/gender and mice.
3. Identification of the best technical solution for a MTS among the examined systems for mice
4. Identification of the best technical solution for a MTS among the examined systems for humans



2. Cooperation between participants

CNR-IEIIT collaborated closely with CNR-IRGB, CNR-ISTEC and SIM for the achievement of D4.1 objectives. In particular, CNR-IRGB provided information about the dimension of the heart and the target area in the small animals, CNR-ISTEC provided information about the size and the magnetic susceptibility of $^{59}\text{FeCaPs}$ whereas SIM provided data on drag force and fluid dynamic parameters for both small animals (mouse) and humans. All these data were then used by CNR-IEIIT to perform the computational simulations of the electromagnetic field distributions in the target area due to the electromagnetic drug targeting systems with the aim to find the best technical solution among the examined systems for both animals and humans applications. Three remote meetings were organized among the participants during the first year of the project to discuss on the approach to be followed and on the results achieved.



3. Computational simulations of electromagnetic fields on heart tissues

3.1. Introduction

Among the many objectives, CUPIDO is envisioned to reach a solid pre-clinical proof of concept by investigating the feasibility of different systems of therapeutic drug delivery to the heart based on two different approaches, i.e. chemical and magnetic targeting. This deliverable focuses on this latter.

Magnetic targeting is a promising technique in which magnetically responsive objects coated by or loaded with therapeutic agents, once reached the blood circulation, are directed to biological targets in the body by externally applied high gradient magnetic fields [Shapiro 2009, Sensening et al. 2012]. This would allow therapy to be concentrated to disease sites (i.e. solid tumors, blood clots, infections) while keeping systemic concentrations low and thus minimizing side effects [Polyak and Friedman, 2009]. The magnetically responsive objects can be micro- or nano-scale iron oxide particles or other particles coated appropriately to be biocompatible and therapeutically effective [Kamaly et al. 2012]. Moreover, those sub-micrometric particles should be small enough to pass from blood to the surrounding tissue through blood vessel walls (in technical terms “extravasate”) and, in realistic applications, their typical radius range between 1 nm-5 μm [Nacev et al. 2011].

The main limitation in magnetic targeting consists in the difficulty to focus such magnetic nanoparticles (MNPs) to target sites, particularly when they are deep inside the body (at distance > 5 cm) [Nacev et al., 2011]. This is due to the minimal magnetic force that can be imposed on MNPs themselves, with a maximum in the order of piconewton (10^{-12} N) for realistic experiments in humans [Nacev et al. 2011]. This magnetic force (F_m) scales, indeed, with the particle volume (in the order of 10^{-27} - 10^{-16} m^3 for MNPs radii in the range 1 nm-5 μm) and rapidly decays with distance from the source (with a similar behavior for both magnets and coils of the same dimension). Additionally, all MNPs are subjected to hydrodynamic forces, that tend to push them away from their target and that, in turn, scale with the particle radius, thus resulting in drag forces several orders of magnitude higher than the corresponding magnetic forces.

Traditional methods based on visual inspection, magnetic resonance imaging, and histology studies used on both animal experiments [Alexiou et al. 2000, Dormer et al. 2008, Goodwin et al. 2001, Marie et al. 2015, Pulfer and Gallo, 1999, Tietze et al. 2012; Ottersbach et al. 2018] and phase I human clinical trials [Lemke et al. 2004, Lubbe et al. 1996a, Lubbe et al. 1996b] have pointed out the accumulation of MNPs in the target areas. This evidence shows that, **under particular conditions**, magnetic forces could enhance the concentration of MNPs in vivo near magnets.

However, one key open issue in magnetic targeting is **whether the applied magnetic forces can face or, at least, approach the convective blood (drag) forces, thus favoring MNPs extravasation**. In other words, which systems maximize the magnetic forces in the target regions against blood flow?

In this deliverable, a computational based approach was used **to analyze and compare the feasibility of different systems in generating the required magnetic gradient field (or magnetic forces) and to optimize magnetic sources for specific drug targeting applications** [Dames et al. 2007; Sarwar et al. 2012; Kilgus et al. 2012]. Then, here, computational electromagnetics techniques have been applied to evaluate the performance of various ad-hoc designed magnetic systems in targeting the heart tissues of differently aged human anatomical models and small animals (mice).

3.1.1. Objectives

To compare, in terms of magnetic field and magnetic forces, the behavior of different systems based on magnets/coils for the guidance of the superparamagnetic version of calcium phosphate nanoparticles (FeCaPs) in the heart tissue, through computational approaches. In particular, the maximum force that each of the examined systems can exert on $\text{FeCaP}/\text{FeCaP}$ agglomerates in the heart



blood vessels has been calculated and then numerically compared to the corresponding drag forces due to the blood flow.

3.2. Material and Methods

3.2.1. Magnetic targeting system (MTS)

The systems generally used in magnetic targeting can be divided in two main categories, both of which present advantages and disadvantages:

- **(Permanent) magnets based systems:** they are the simplest technical solution for MTS. They are made of a ferromagnetic material, which is magnetized by a strong external magnetic system able to create a persistent magnetic field. Neodymium magnets are the strongest type of permanent magnet commercially available. On the other hand, these magnets have upper limits in both maximum persistent magnetic field and size (< 10 cm radius) and they cannot be “switched off” if necessary.
- **Coils (electromagnets) based systems:** they are made from a coil of wire that acts as a magnet when an electric current passes through it. Often an electromagnet is wrapped around a core of ferromagnetic material like steel, which enhances the magnetic field produced by the coil itself. The main advantage of an electromagnet over a permanent magnet is that it can be rapidly manipulated over a wide range by controlling the amount of electric current supplied and hence they are more prone to guide and focus MNPs through a closed-loop control. On the other hand, these systems need of a continuous supply of electrical energy and require very high current level (with the related technical issues such as Joule heating, induction of electric field in the conductive media, including body, power electronics, ...) to reach the magnetic field levels generated by the static counterpart.

Given the above and the similar behavior of the two system categories, we focused first on solutions based on magnets, and then moved to coils based systems, calculating the current needed in coils of the same dimension as magnets to generate the same magnetic force.

3.2.1.1. Modelling of Magnetic fields and Forces

The propagation through the space of magnetic fields generated by a magnetic targeting system MTS is described by the Maxwell's equation. For static and slowly time-varying magnetic fields, the magneto quasi-static approximation is applied:

$$\nabla \times \vec{H} = \vec{j} \quad (1)$$

$$\nabla \cdot \vec{B} = 0 \quad (2)$$

$$\vec{B} = \mu_0(\vec{H} + \vec{M}) = \mu_0(\vec{H} + \chi\vec{H}) \quad (3)$$

Where \vec{B} is the magnetic induction [in units of Tesla T], \vec{H} is the magnetic field [A/m], \vec{M} is the material magnetization [A/m], $\mu_0=4\pi \cdot 10^{-7}$ N/A² is the vacuum permeability, $\chi=(\mu_r-1)$ is the magnetic susceptibility and μ_r is the relative magnetic permeability. These equations hold both in vacuum and in materials and for both permanent magnets (magnetization $\vec{M} \neq 0$) and electromagnets (current $\vec{j} \neq 0$) and have been here numerically solved through the magneto static solver as implemented by simulation platform CST EM Studio [CST, Darmstadt, Germany] and through the magneto quasi-static solver of simulation platform SEMCAD X [by SPEAG, Zurich, Switzerland].

Magnetic fields pass virtually unchanged through the human tissues because their magnetic susceptibility χ is close to zero. In contrast, the cores of ferromagnetic MNPs have magnetic susceptibilities several orders of magnitude higher than that of tissue, resulting in strong interactions with external magnetic fields.

Magnetic force (F_m) on a single spherical MNP or MNP agglomerate depends on both magnetic field and magnetic field gradient created at its location by an external MTS and is given by:



$$\vec{F}_m = \frac{4\pi a^3}{3} \frac{\mu_0 \chi}{(1+\frac{\chi}{3})} \vec{H} \frac{d\vec{H}}{d\vec{x}} = \frac{2\pi a^3}{3} \frac{\mu_0 \chi}{(1+\frac{\chi}{3})} \nabla (|\vec{H}|^2) = C_F \nabla (|\vec{H}|^2) \quad (4)$$

where a is the radius of the MNP/MNP agglomerate, $\vec{x}=(x,y,z)$ is its location, and $\nabla = (\frac{d}{dx}, \frac{d}{dy}, \frac{d}{dz})$ is the spatial gradient operator and $C_F = \frac{2\pi a^3}{3} \frac{\mu_0 \chi}{(1+\frac{\chi}{3})}$ is the coefficient which multiplies the gradient of squared magnetic field and depends only on physical factors of the MNP.

F_m distribution was calculated from magnetic field distribution through a MATLAB [The MathWorks, Natick, MA] code.

Equation 4 shows that:

- **the magnetic force scales with the particle volume.**
- **A spatially varying magnetic field $\frac{d\vec{H}}{d\vec{x}} \neq 0$ is required to create a magnetic force**
- The gradient operator points from low to high regions of the squared magnetic field, which means that MNPs experience forces from low to high applied magnetic field and hence that **magnetic systems always attract** them.

3.2.2 Blood Forces

Besides magnetic force, there are several other forces acting on any particle moving in blood vessels. Those include drag forces, Brownian force, thermophoresis force, Saffman's lift force, Magnus force and Basset force. Due to different assumption, as explained in the paper by Pourmehran and colleagues [Pourmehran et al., 2015], all but drag force can be neglected and the motion of the considered MNPs in blood vessels can be described by the following equation:

$$\sum \vec{F} = m_{NP} \frac{dv_{NP}}{dt} = \vec{F}_d + \vec{F}_m \quad (5)$$

where v_{NP} is the MNP velocity, m_{NP} its mass, F_m the magnetic force as in Eq. (4), and F_d is the hydrodynamic **drag force**, which is, for spherical MNP/agglomerate, given by the following **Stokes' law** [Pourmehran et al. 2015, Tehrani et al. 2014]:

$$\vec{F}_d = -6\pi\eta a(\vec{v}_{NP} - \vec{v}_b) \quad (6)$$

where η is the blood viscosity and v_b is the blood velocity. **Using the centerline blood velocity to estimate the drag forces dramatically overestimates these forces near the vessel walls, and thus severely under-predicts the ability of magnetic drug targeting to capture particles** [Nacev et al. 2012]. Thus, according to Nacev and colleagues, we compared the magnetic force (F_m) both with the:

- F_d (centerline), which is the drag force estimated with the centerline blood velocity (i.e. the highest fluid velocity as calculated at the center of the vessel);
- F_d (boundary), which is the drag force estimated in the boundary layer, which is, in turn, the 0.1% of the centerline velocity.

By solving Eq. (5) the trajectory of MNPs can be calculated. However, the solution of this differential equation is out of the scope of this report and in the following, we will **discuss the force balance at the equilibrium, namely the numerical comparison between the drag forces due to the blood velocity and the magnetic force F_m .**

3.2.3 Target area definition

Medications used to treat cardiovascular disorders are typically delivered to heart through the coronary arteries, which are the vessels that directly supply blood to the myocardium and to other components of the heart [Scott et al. 2008]. As a consequence, the target area of MTS should be at the coronary circulation level.



In humans, two different approaches have been investigated, both of which are aimed to target $^{59}\text{FeCaPs}$ in the coronary circulation. With the first approach we tried to guide MNPs from the aortic valve to the entrance of the coronary arteries in order to increase their concentration in the coronary circulation. With the second approach, we wanted to extend the retention of MNPs through coronary capillaries walls, by maximizing their permanence in the small vessels themselves. In the following section, we will show that the first approach cannot be reached through a feasible MTS whereas the second is more achievable in both humans and mice.

3.2.1.2. Target area definition in humans

Coronary circulation occurs mainly during diastole (**Error! Reference source not found.**).

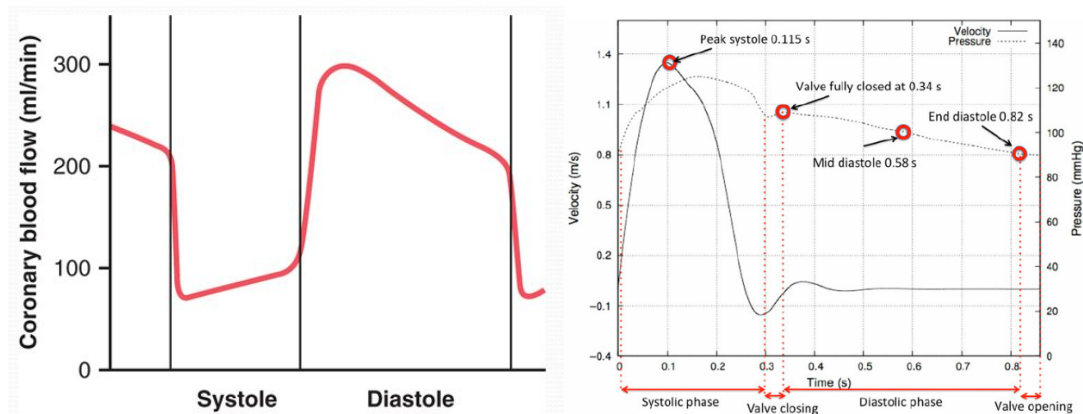


Figure 1 Coronary blood flow (left) and aorta blood velocity (right) during a cardiac cycle. Redrawn from Hall [2011]

During systole, the subendocardial coronary vessels are compressed due to the high ventricular pressures. This compression results in momentary retrograde blood flow (i.e., the blood flows backward toward the aorta), which further inhibits perfusion of myocardium during systole (i.e., the blood flow in the subendocardium stops). As a result, most myocardial perfusion occurs during diastole when the subendocardial coronary vessels are open and under lower pressure. For this reason, magnetic targeting should occur during systolic phase. In other words, in order to maximize the entrance of MNPs in the coronaries, the MTS should be able to affect $^{59}\text{FeCaPs}$ (in terms of increasing the likelihood of MNPs shifting towards the coronary vessels) between the aortic valve and the entrance of the coronary arteries (that are few mm above) during systole and leave them go through (by switching off the MTS) the coronary arteries during diastole.

Permanent magnets, by generating a static magnetic field, are not prone to this purpose, whereas electromagnets synchronized with the heart cycle should be used. However, two issues make this problem hard to solve:

- 1) The blood velocity in the aorta can reach up to 1.2 m/s (**Error! Reference source not found.**) and hence we would need to set a magnetic force of the order of $F_m = 2 \cdot 10^{-8} \text{ N}$;
- 2) The distance between skin surface (where the MTS could be positioned) and the target area (coronary arteries entrance) is of about 6 cm in adults and as discussed above, F_m amplitude is proportional to the squared amplitude of the magnetic field, which, in turn, decrease with an inverse cube law respect to the distance.

As a result, we would need a coil which produce a very high magnetic induction (in the order of hundreds of T), which means, for coils with radii in the range 5-10 cm, a current per turn very high (in the order of 10^6 A), which clearly indicates a not feasible solution.

Given these results, it was decided to design the MTS as a device that was able, by attracting MNPs towards itself, **to enhance the $^{59}\text{FeCaP}$ concentration in the heart area and to favor the extravasation of the $^{59}\text{FeCaPs}$ from coronary capillaries to the myocardium.** The target area was confirmed to be only the coronary capillaries where the direct feeding of the myocardium tissue occurs and where:



- given the lower blood velocity in human capillaries, the drag forces that MTS should face are considerably lower than in the aorta;
- given the shorter distance of the coronary capillaries than aorta from the skin surface, the MTS can exert a considerably higher magnetic force than in the aorta;
- there is no more the need to synchronize the magnetic force with the heartbeat and hence it is possible to explore the use of permanent magnets based systems.

The anatomical models used in the simulations come from the Virtual Population models [Christ et al. 2010, Gosselin et al. 2015] made available to CNR-IEIIT for research purpose from IT'IS Foundation (Zurich, Switzerland). The models are based on high-resolution magnetic resonance (MR) images of healthy volunteers, segmented in a voxel-based format and reconstructed through the use of computer-aided design representation of the organ surfaces. Up to 84 tissues are distinguished in the whole body models whereas, at the heart level, it is possible to distinguish the heart lumen, the heart muscle (myocardium) and the largest blood vessels.

The minimum target area distance D_{target} (i.e. the minimum distance between the coronary capillaries and the skin surface), ranges between 10 and 32 mm across the human models.

3.2.1.3. Target area definition in small animals

The performance evaluation of different MTS in exerting a magnetic force opposing to the blood drag forces was been computationally evaluated also for small animal models. In particular, here we focused on mice, since used in CUPIDO animal experiments.

All anatomical data referred to mouse were provided by CNR-IRGB. According to those, for mouse the minimum target area distance D_{target} (the distance between the coronary capillaries and the skin surface) is of about $D_{\text{target}}=2$ mm.

3.2.4 Magnetic targeting system (MTS) and simulation details

Bearing in mind that MTS is thought to act on heart tissue, its dimensions were chosen accordingly. Magnetic targeting systems examined consist in a single disc magnet/round coil, given that either multiple or different shapes do not substantially change our results (data here not shown). The studied systems are therefore modelled as single circular magnets.

A uniform axial permanent magnetization (or remanence) was set to disc magnets in the simulation according to the maximum B_r of commercially available magnets. The current in a single coil of one turn ($N=1$) with the same radius as magnet was calculated to have at the loop center the same maximum magnetic field induction at the central point of the upper face magnet center, through the well-known Biot-Savart equation:

$$NI = \frac{2R_{\text{coil}}B_{\text{center}}}{\mu_0} \quad (7)$$

Magnetic targeting systems were placed on the skin tissue of each model at the heart level, with their center at the level of the heart center and with a minimum distance from the heart surface equal to the minimum target distance. Computational domain was discretized using a uniform rectilinear mesh grid. The magnetic field distribution in the space below the MTS was extracted from the electromagnetic simulator and then imported in MATLAB to calculate the magnetic force distribution.

3.3. Results

3.3.1. Magnetic force in mice



As discussed above, we first calculated the maximum F_m generated by single disc magnet based systems with variable radius at the target distance on a $FeCaP$ agglomerate. The maximum F_m obtained varying the radius of the magnets are about 20% lower than the maximum blood drag force but hundreds times higher than the minimum (boundary layer) blood drag force calculated in the mouse coronary capillaries.

Then we calculated the current (per single turn) supplied to the coil based system of the same dimension as magnets in order to produce the same F_m calculated for magnet. Our results show that they would need a very high feeding current (in the order of thousands A-turn) to equal the force exerted by magnets of the same size.

Lately, some studies [Tehrani et al. 2014, Han et al. 2012, Martel et al. 2009] have used a combination of particular coils arrangement, namely Helmholtz and Maxwell coils, for MNP guidance into blood vessels model. Both coils arrangements consist of two identical circular coils (radius= R) placed symmetrically along their central axis and separated by a distance $z=R$. Each coil carries an equal electric current I :

- ✓ In the same direction in **Helmholtz** coils, that are used for producing an almost uniform **H** (or **B**) and then an almost **null** F_m in the volume interposed between them;
- ✓ In the opposite direction in gradient-**Maxwell** coils, used for producing a uniform-gradient magnetic field **H** (or **B**) and an almost **linear** $F_m(z)$, in the volume between them.

By adding the two coils set together, the superimposition of their **B** would allow to apply a non-zero magnetic force on the MNPs, wherever they are placed in the volume interposed between the two coils of each pair.

The behavior of a hypothetical and ideal Helmholtz+Maxwell coil system, to be used in experiments on mice, was evaluated. The distance between the coils and equally the coils radius was set to the mouse thorax width (**Error! Reference source not found.**). We then calculated the current (per single turn) in each coil of the Helmholtz+Maxwell system needed to produce at the target distance:

- the same F_m calculated for a single disc magnet system of the same dimension.
- the maximum F_m calculated for single disc magnet system

In both cases, the feeding current still results quite high.

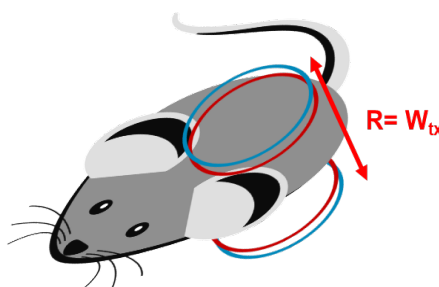


Figure 2 Pictorial representation of the Helmholtz+Maxwell Coils system

More detailed information are not included here since part of a manuscript in preparation.

3.3.2 Magnetic force in humans

Similarly to mice, the computational analysis of the magnetic targeting system MTS in humans starts from single disc magnet based systems. Given the different target distance, due to the different anatomical characteristics of human models, the best magnet based solution varies across human models. The maximum F_m obtained for each human model are about the 5-10% of the centerline (or maximum) drag force, but are about tens times higher than the boundary layer (or minimum) drag force calculated in the human coronary capillaries.



As for mice, we calculated the current (per single turn) supplied to a coil based MTS in order to produce the maximum F_m calculated for magnets. As expected, the results are even worse than what found for mice. Even if, hypothetically, coils can be manufactured as larger as desired, the feeding current needed is too high and clearly not feasible for our purposes.

More detailed information are not included here since part of a manuscript in preparation.

4. Conclusions

In summary, the analysis of the capability of different magnetic targeting systems based on magnets and coils in reaching the heart with a **force that would compete with the blood drag force**, thus **favoring the absorption of ^{Fe}CaP agglomerates in the heart tissues**, shows that:

- For **mice**, systems based on small commercially available **magnets** seem to be capable to generate enough force to slow down NPs speed locally and then to **enhance the absorption of a large fraction of $^{Fe}CaPs$ through capillaries walls**.
- For **humans**, actually commercially available **magnets based systems** (with an optimum radius depending of the individual anatomy) **represent the best solution** in terms of possible depth of targeting, cost, complexity and ease-of-use. They allow **attracting the slowest $^{Fe}CaPs$ towards anterior and superficial coronary capillaries walls**, but are probably less effective on $^{Fe}CaPs$ that moves at higher velocities.



5. References

- Alexiou C, Arnold W, Klein R J, Parak F G, Hulin P, Bergemann C, Erhardt W, Wagenpfeil S and Lubbe A S2000 Locoregional cancer treatment with magnetic drug targeting *Cancer Res.* **60** 6641–8
- Briers JD, Webster S. 1996. Laser speckle contrast analysis (LASCA): a non-scanning, full-field technique for monitoring capillary blood flow. *J Biomed Opt.* **1**(2): 174–179. doi: 10.1117/12.231359
- Cassar, A., Holmes, D. R., Rihal, C. S., & Gersh, B. J. (2009). Chronic Coronary Artery Disease: Diagnosis and Management. *Mayo Clinic Proceedings*, *84*(12), 1130–1146. <http://doi.org/10.4065/mcp.2009.0391>
- Christ, A.; Kainz, W.; Hahn, E.G.; Honegger, K.; Zefferer, M.; Neufeld, E.; Rascher, W.; Janka, R.; Bautz, W.; Chen, J.; et al. The virtual family-development of surface-based anatomical models of two adults and two children for dosimetric simulations. *Phys. Med. Biol.* **2010**, *55*, 23–38.
- Dames P, Gleich B, Flemmer A et al. "Targeted delivery of magnetic aerosol droplets to the lung" *Nat Nanotechnol.* **2007 Aug**; *2*(8): 495–499. Published online 2007 Jul 22. doi: 10.1038/nnano.2007.217
- Dormer KJ, Awasthi V, Galbraith W, Kopke RD, Chen K, Wassel R. Magnetically-targeted, technetium 99m-labeled nanoparticles to the inner ear. *J. Biomed. Nanotechnol.* **2008**; *4*(2):174–184.
- Earnshaw S, "On the nature of the molecular forces which regulate the constitution of the luminiferous ether," *Trans. Cambridge Philos. Soc.*, vol. 7, no. 1, pp. 97–112, 1842.
- Goodwin S C, Bittner C A, Peterson C L and Wong G 2001 Single-dose toxicity study of hepatic intra-arterial infusion of doxorubicin coupled to a novel magnetically targeted drug carrier *Toxicol. Sci.* **60** 177–83 *J. Neuro-Oncol.* **41** 99–105
- Gosselin MC et al. 2014. Development of a new generation of high-resolution anatomical models for medical device evaluation: the Virtual Population 3.0. *Phys Med Biol.* **2014 Sep 21**; *59*(18):5287-303. doi: 10.1088/0031-9155/59/18/5287. Epub 2014 Aug 21.
- X. Han, Q. Cao, and L. Li, "Design and evaluation of three-dimensional electromagnetic guide system for magnetic drug delivery," *IEEE Trans. Appl. Supercond.*, vol. 22, no. 3, pp. 1–32, Jun. 2012.
- Kamaly N, Xiao Z, Valencia PM, Radovic-Moreno AF, Farokhzad OC. Targeted polymeric therapeutic nanoparticles: design, development and clinical translation. *Chemical Society reviews.* **2012**; *41*(7):2971-3010. doi:10.1039/c2cs15344k.
- Kilgus C, Heidsieck A, Ottersbach A, Roell W, Trueck C, Fleischmann BK, Gleich B, Sasse P 2012 Local gene targeting and cell positioning using magnetic nanoparticles and magnetic tips: comparison of mathematical simulations with experiments. *Pharm Res.* **2012 May**; *29*(5): 1380–1391. Published online 2011 Dec 30. doi: 10.1007/s11095-011-0647-7
- Lemke AJ, von Pilsach MIS, Lubbe A, Bergemann C, Riess H, Felix R. MRI after magnetic drug targeting in patients with advanced solid malignant tumors. *European Radiology* **Nov;2004 14**:1949–1955. [PubMed: 15300401]
- Lubbe AS, Bergemann C, Huhnt W, Fricke T, Riess H, Brock JW, Huhn D. Preclinical experiences with magnetic drug targeting: Tolerance and efficacy. *Cancer Research* **Oct 15;1996 56**:4694–4701 [PubMed: 8840986]
- Lubbe AS, Bergemann C, Riess H, Schriever F, Reichardt P, Possinger K, Matthias M, Dorken B, Herrmann F, Gurtler R, Hohenberger P, Haas N, Sohr R, Sander B, Lemke AJ, Ohlendorf D, Huhnt W, Huhn D. Clinical experiences with magnetic drug targeting: A phase I study with 4'-epidoxorubicin in 14 patients with advanced solid tumors. *Cancer Research* **Oct 15;1996 56**:4686–4693. [PubMed: 8840985]
- Marie, H. et al. Superparamagnetic liposomes for mri monitoring and external magnetic field-induced selective targeting of malignant brain tumors. *Adv. Funct. Mater.* **25**, 1258–1269 (2015).
- Martel S et al., "MRI-based medical nanorobotic platform for the control of magnetic nanoparticles and flagellated bacteria for target interventions in human capillaries," *Int. J. Robot. Res.*, vol. 28, no. 9, pp. 1169–1182, Sep. 2009
- Nacev A., Beni C., Bruno O., Shapiro B. The behaviors of ferromagnetic nano-particles in and around blood vessels under applied magnetic fields. *J. Magn. Magn. Mater.* **2011**; *323*:651–668
- Ottersbach A, Mykhaylyk O, Heidsieck A, et al. Improved heart repair upon myocardial infarction: Combination of magnetic nanoparticles and tailored magnets strongly increases engraftment of myocytes. *Biomaterials.* **2017 Nov 15**; *155*:176-190. doi: 10.1016/j.biomaterials.2017.11.012. [Epub ahead of print]
- Q. A. Pankhurst, N. K. Thanh, S. K. Jones, and J. Dobson, "Progress in applications of magnetic nanoparticles in biomedicine," *J. Phys. D: Appl. Phys.*, vol. 42, no. 22, pp. 224,001–224,016, 2009
- Pulfer S K and Gallo J M 1999 Enhanced brain tumor selectivity of cationic magnetic polysaccharide microspheres *J. Drug Targeting* **6** 215–28
- Polyak B, Friedman G: Magnetic targeting for site-specific drug delivery: applications and clinical potential. *Expert Opin Drug Deliv.* **2009 Jan**; *6*(1): 53–70. doi: 10.1517/17425240802662795
- Pourmehrhan O, Rahimi-Gorji M, Gorji-Bandpy M, Gorji TB. Simulation of magnetic drug targeting through tracheobronchial airways in the presence of an external non-uniform magnetic field using Lagrangian magnetic particle tracking, *Journal of Magnetism and Magnetic Materials.* vol.393, pp. 380-393
- Sarwar A, Nemirovski A, Shapiro B. 2012. Optimal Halbach Permanent Magnet Designs for Maximally Pulling and Pushing Nanoparticles *J Magn Magn Mater.* **324**(5): 742–754. Published online 2011 Sep 19. doi: 10.1016/j.jmmm.2011.09.008



Scott RC, Crabbe D, Krynska B, Ansari R, Kiani MF. Aiming for the heart: targeted delivery of drugs to diseased cardiac tissue. *Expert Opin Drug Deliv.* 2008 Apr; 5(4): 459–470. doi: 10.1517/17425247.5.4.459

Sensenig R, Sapir Y, MacDonald C, Cohen S, Polyak B. Magnetic nanoparticle-based approaches to locally target therapy and enhance tissue regeneration in vivo. *Nanomedicine (London, England).* 2012;7(9):1425-1442. doi:10.2217/nnm.12.109.

Shapiro B. Towards dynamic control of magnetic fields to focus magnetic carriers to targets deep inside the body. *Journal of Magnetism and Magnetic Materials.* 2009;321(10):1594.

Shapiro B, Kulkarni S, Nacev A, Muro S, Stepanov PY, Weinberg IN. Open challenges in magnetic drug targeting. *Wiley Interdiscip Rev Nanomed Nanobiotechnol.* 2015 May-Jun;7(3):446-57. doi: 10.1002/wnan.1311. Epub 2014 Nov 6.

Tehrani MD, Kim MO, Yoon J. A Novel Electromagnetic Actuation System for Magnetic Nanoparticle Guidance in Blood Vessels. *IEEE Transactions on Magnetics* 2014, vol. 5(7), n.5100412

Tietze, R., Lyer, S., Dürr, S. & Alexiou, C. Nanoparticles for cancer therapy using magnetic forces. *Nanomedicine* 7, 447–457 (2012).